Journal of Solid State Chemistry 184 (2011) 3144–3149

Contents lists available at SciVerse ScienceDirect

Journal of Solid State Chemistry

journal homepage: www.elsevier.com/locate/jssc

Solvothermal synthesis of a bimetallic thiometallate containing germanium in two oxidation states

Anthony V. Powell*, Rosalyn Mackay

Department of Chemistry, Heriot-Watt University, Edinburgh EH14 4AS, UK

ARTICLE INFO

Article history:
Received 6 July 2011
Received in revised form
21 September 2011
Accepted 24 September 2011
Available online 4 October 2011

Keywords:
Thiometallates
Chalcogenides
Crystal structure
Solvothermal
Optical properties

ABSTRACT

A new layered germanium–antimony sulphide, $[Ge(C_2N_2H_8)_3][GeSb_2S_6]$, has been prepared at 463 K under solvothermal conditions in the presence of ethylenediamine. The compound has been characterised by single-crystal X-ray diffraction, thermogravimetry, elemental analysis and reflectance spectroscopy. $[Ge(C_2N_2H_8)_3][GeSb_2S_6]$ crystallises in the space group *Pbca* (a=13.3284(5), b=17.4801(6), c=18.5447(7) Å). The structure consists of cyclic $[GeSb_2S_8]^{6-}$ units that form chains which are cross-linked through Sb_2S_2 rings to generate layers of stoichiometry $[GeSb_2S_6]^{2-}$, between which $[Ge(en)_3]^{2+}$ cations are located. $[Ge(C_2N_2H_8)_3][GeSb_2S_6]$ contains germanium in both the divalent and tetravalent states. The optical band gap of 2.49(4) eV is in excellent agreement with the value expected on the basis of the correlation with the density of metal centres previously identified for thioantimonates, and is consistent with states at the top of the valence band being predominantly of sulphur 3*p* character.

1. Introduction

Template-directed synthesis is increasingly used for the synthesis of inorganic and hybrid materials with novel architectures. Originally applied to the laboratory synthesis of zeolites and aluminosilicates, the approach was extended to tin and germanium sulphides by Bedard et al. [1]. Subsequently, there has been a tremendous growth of interest in the use of template-directed synthesis of main-group chalcogenides [2]. The primary building units in materials containing elements from groups 13 and 14 are metal-centred tetrahedra [3–5]. Furthermore, in the case of indium- and gallium-containing materials, vertex-linking of tetrahedral MS_4 units can give rise to supertetrahedral clusters [6], which may themselves serve as building blocks for the construction of complex structures. A recent development has been the demonstration that functionalisation of the vertices of supertetrahedra provides a means of connecting such units through organic linkers, giving rise to unusual hybrid frameworks [7,8].

By contrast, the chemistry of antimony sulphides is dominated by trigonally–pyramidally coordinated SbS_3 units in which the lone-pair of electrons is stereochemically active. The different coordination preferences of antimony compared to its group 13 and 14 congeners manifest itself in a preponderance of chain-like [2,9] and layer-type [10] structures amongst the antimony sulphides. Longer-range interactions, which increase the effective coordination number of antimony, are also commonly present in these structures. Such interactions may serve to link one- and two-dimensional units into structures of higher dimensionality [10]. Moreover, we have recently shown that antimony sulphides may also adopt three-dimensional framework structures in which the connectivity is exclusively through primary Sb–S bonding [11,12]: a three-dimensional framework is also observed in $K_2Sb_4S_7$ prepared hydrothermally [13].

Synthesis of these materials is generally effected in the presence of organic amines as structure-directing agents. These are principally linear and branched long-chain aliphatic amines or polyamines or alicyclic amines. The instability of long-chain polyamines at elevated temperatures [14] provides further geometric diversity as they can undergo side-reactions such as cyclisation [15] and cleavage [9(e)]. Furthermore, the addition of transition-metal cations to the solvothermal reaction mixture can lead to the formation of cationic coordination complexes which also appear to play a role in directing the crystallisation of the main-group sulphide matrix [3]. The products of solvothermal reaction in the presence of an organic amine generally consist of complex anionic metal–sulphide frameworks with protonated amines or cationic transition-metal complexes fulfilling the charge-balancing role. In favourable cases [16–20], the transition-metal may also be incorporated into the primary-bonded metal-sulphide network, introducing a further degree of structural diversity.

A promising approach for the generation of new structure types is to introduce two metals with different coordination

* Corresponding author. Fax: +44 131 451 3180.
E-mail address: a.v.powell@hw.ac.uk (A.V. Powell).

0022-4596/$ - see front matter © 2011 Elsevier Inc. All rights reserved.
doi:10.1016/j.jssc.2011.09.032

preferences into the solvothermal reaction mixture, effectively combining two different structural building blocks [21–25]. For this reason, we have recently begun to explore the use of mixtures of main-group metals for solvothermal synthesis in the presence of linear polyamines. Here, we report the synthesis of the new layered material, $[Ge(C_2N_2H_8)_3][GeSb_2S_6]$, whose bimetallic thiometallate layers are constructed from three- and four-coordinate antimony and tetrahedrally coordinated germanium in a similar fashion to that of the recently reported $[M(C_2N_2H_8)_3][GeSb_2S_6]$ (M=Ni, Co) [26]. This material unexpectedly contains germanium in both the +2 and +4 oxidation states.

2. Experimental

2.1. Synthesis

Single crystals of $[Ge(C_2N_2H_8)_3][GeSb_2S_6]$ were prepared under solvothermal conditions. GeO_2 (0.31 g; 3 mmol), Sb_2S_3 (0.51 g; 1.5 mmol) and S (0.24 g; 7.5 mmol) were added to 5 mL (70 mmol) of ethylenediamine in a Teflon-lined stainless steel autoclave (23 mL) to form a mixture of molar composition GeO_2:Sb_2S_3:S:en of 6:3:15:140. The mixture was stirred at room temperature for 15 min prior to sealing the autoclave. The autoclave was placed in an oven at room temperature and heated at a rate of 2 K min^{-1} to 463 K. After 6 days at this temperature, the oven was cooled to room temperature at 2 K min^{-1}. The solid product (approximate yield 80%) was filtered, washed with ethylenediamine and dried in air at room temperature. The product consisted of crystals, in the form of yellow blocks, of the title compound, together with trace amounts of black powder.

2.2. Characterisation

Powder X-ray diffraction data on a ground portion of the bulk sample (Figure S1 of the Supplementary materials) were collected using a Bruker D8 Advance powder diffractometer, operating with germanium-monochromated Cu$K\alpha_1$ radiation (λ=1.5405 Å) and fitted with a Bruker LynxEye^{TM} linear detector. All peaks in the diffraction pattern can be indexed on the basis of the orthorhombic unit cell determined from the single-crystal diffraction study, with refined lattice parameters a=13.339(1), b=17.497(2), c=18.561(2) Å that are in good agreement with those determined from the single-crystal study, indicating that the sample is essentially monophasic. No reflections could be identified as arising from the trace amount of black powder, indicating that it is either amorphous to X-rays or is present in too small a quantity to make any appreciable contribution to the X-ray profile. Indexing and lattice parameter refinement was carried out using the Topas package. Combustion analysis of hand-picked single crystals gave C 10.91, H 3.37 and N 11.63% which compares favourably with the values calculated from the crystallographically determined formula $[Ge(C_2N_2H_8)_3][GeSb_2S_6]$ (C 9.47, H 3.18 and N 11.04%). Thermogravimetric analysis (Figure S2 of the Supplementary materials) was performed using a DuPont Instruments 951 thermal analyser. Approximately 12.5 mg of finely ground crystals was heated under a flow of oxygen over the temperature range 30–1000 °C at a heating rate of 10 °C min^{-1}. The weight loss of 2.48% that occurs below 100 °C may be assigned to a residual solvent on the surface of the sample. This is followed by a weight loss of 33.7% that occurs in two overlapping steps, with onset temperatures of *ca.* 189 °C and 405 °C. This weight change is in very good agreement with that calculated (32.1%) for the loss of three ethylenediamine ligands and conversion of the metal sulphide to a mixture of GeO_2 and Sb_2O_4, which was identified in the product of thermogravimetric analysis by powder X-ray diffraction (Figure S3 of the Supplementary materials).

Table 1
Crystallographic data for $[Ge(C_2N_2H_8)_3][GeSb_2S_6]$.

Formula	$[Ge(C_2N_2H_8)_3][GeSb_2S_6]$
M_r	761.36
Crystal habit	Yellow block
Dimensions (mm)	0.22 × 0.28 × 0.37
Crystal system	Orthorhombic
Space group	*Pbca*
T (K)	293
a (Å)	13.3284(5)
b (Å)	17.4801(6)
c (Å)	18.5447(7)
V (Å^3)	4320.6(3)
Z	8
Wavelength (Å)	0.71073
μ (cm^{-1})	5.813
Measured data	63047
Unique data	4424
Observed data ($I > 3\sigma(I)$)	3280
R_{merg} (%)	3.40
R (%)	3.13
R_w (%)	3.47

Diffuse reflectance data were measured over the frequency range 9090–50,000 cm^{-1} using a Perkin Elmer, Lambda 35 UV–vis spectrometer. $BaSO_4$ was used as a reference material. Measurements were made on *ca.* 10 mg of finely ground hand-picked crystals, diluted with $BaSO_4$. The band gap was determined by applying the Kubelka–Munk function and extrapolating the linear portion of the absorption edge to the energy axis [27].

X-ray intensity data for crystals of $[Ge(C_2N_2H_8)_3][GeSb_2S_6]$ were collected at 293 K using a Bruker Nonius X8 Apex diffractometer with Mo$K\alpha$ radiation (λ=0.71073 Å) and data were processed using the Apex-2 software [28]. The structure was solved by direct methods using the program SIR-97 [29], which located all of the Ge, Sb and S atoms. Subsequent Fourier calculations and least-square refinements on F were carried out using the CRYSTALS program suite [30]. The C and N atoms of the coordinated amine were located in a difference Fourier map. Hydrogen atoms were placed geometrically on the C and N atoms after each cycle of refinement. In the final cycle of refinement, all non-hydrogen atoms were refined anisotropically. Crystallographic and refinement details are given in Table 1.

3. Results and discussion

The atomic coordinates and equivalent isotropic thermal parameters of non-hydrogen atoms of $[Ge(C_2N_2H_8)_3][GeSb_2S_6]$ are given in Table 2. Fig. 1 shows the local coordination of the atoms, while selected bond lengths and angles are presented in Table 3. The structure consists of anionic germanium–antimony sulphide layers and charge balancing germanium tris (ethylenediamine) complexes. Within the anionic framework there are two crystallographically distinct antimony atoms and one germanium atom. The latter has a slightly distorted tetrahedral geometry with the four Ge(1)–S distances lying in the range 2.136(2)–2.262(1) Å. Of the two antimony atoms, Sb(1) is approximately trigonally–pyramidally coordinated by sulphur, with three short Sb–S distances in the range 2.427(2)–2.468(1) Å. However, as is commonly observed in templated antimony sulphides, there are two additional longer-range Sb–S interactions (Sb(1)–S(1): 3.466(1) Å; Sb(1)–S(3): 3.141(1) Å) that are within the sum of the van der Waals' radii of Sb and S [31]. Sb(2) is four coordinate with two short and two longer bonds to sulphur. SbS_4^{5-} units with this

Table 2
Fractional atomic coordinates and equivalent isotropic thermal parameters (Å^2) for non-hydrogen atoms in $[Ge(C_2N_2H_8)_3][GeSb_2S_6]$.

Atom	*x*	*y*	*z*	U_{iso}
Sb(1)	0.23754(2)	0.09759(2)	0.30605(2)	0.0229
Sb(2)	0.00891(3)	0.02167(2)	0.40386(2)	0.0272
Ge(1)	−0.00428(3)	0.11354(3)	0.22246(3)	0.0216
Ge(2)	0.21766(6)	0.69128(4)	0.59403(4)	0.0469
S(1)	−0.0475(1)	0.19473(9)	0.14219(8)	0.0386
S(2)	−0.1168(1)	0.01792(8)	0.2272(1)	0.0399
S(3)	0.01948(9)	0.15978(7)	0.33230(6)	0.0250
S(4)	0.1401(1)	0.04853(9)	0.20339(7)	0.0368
S(5)	0.1925(1)	0.00561(9)	0.39858(8)	0.0384
S(6)	−0.0127(1)	0.10064(7)	0.50777(7)	0.0311
N(1)	0.2245(4)	0.8165(3)	0.5889(3)	0.0352
N(2)	0.2830(4)	0.7088(3)	0.4853(3)	0.0435
N(3)	0.2033(3)	0.5682(3)	0.5681(3)	0.0320
N(4)	0.0617(4)	0.6861(3)	0.5531(3)	0.0352
N(5)	0.3554(4)	0.6721(3)	0.6566(3)	0.0436
N(6)	0.1574(4)	0.6834(3)	0.7065(3)	0.0395
C(1)	0.2901(4)	0.8398(3)	0.5289(3)	0.0370
C(2)	0.2738(5)	0.7899(4)	0.4640(3)	0.0425
C(3)	0.1045(5)	0.5526(3)	0.5364(3)	0.0402
C(4)	0.0279(4)	0.6071(3)	0.5657(4)	0.0387
C(5)	0.2355(6)	0.6592(4)	0.7571(4)	0.0516
C(6)	0.3356(6)	0.6901(4)	0.7328(4)	0.0524

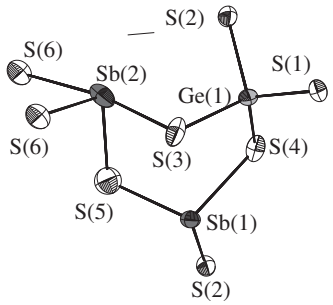

Fig. 1. Local coordination of the framework atoms showing the atom labelling scheme and thermal ellipsoids at 50% probability.

"2+2" coordination have been observed in a number of thioantimonates [11,12,32–34] and have a coordination geometry that may be considered to be derived from that of a trigonal bipyramid by removal of one of the equatorial ligands, resulting in a distorted see-saw-like geometry.

The trigonal pyramidal $Sb(1)S_3^{3-}$ primary building unit shares a common sulphur vertex (S(4)) with the $Ge(1)S_4$ tetrahedron and another (S(5)) with the $Sb(2)S_4$ unit. The latter is also linked to GeS_4 via S(3) to complete a six-membered $GeSb_2S_3$ heteroring, with a boat-like conformation, within a $[GeSb_2S_8]^{6-}$ secondary building unit (Fig. 1). Individual $[GeSb_2S_8]^{6-}$ building units are connected through the exocyclic S(2) that is common to Sb(1) and Ge(1), to form an undulating chain of stoichiometry $[GeSb_2S_7]^{4-}$ directed approximately parallel to [100] (Fig. 2). Pairs of $Sb(2)S_4$ units in neighbouring chains, share common edges, to form Sb_2S_2 rings that serve to link individual $[GeSb_2S_7]^{4-}$ chains into layers of stoichiometry $[GeSb_2S_6]^{2-}$ that lie within the *ac* crystallographic plane (Fig. 3). These layers contain large $Ge_4Sb_8S_{12}$ heterorings, with dimensions of approximately 8.7 × 13.5 Å (measured from atom to atom). This suggests a maximum effective aperture of *ca.* 5 × 10 Å when the van der Waals' radius of sulphur is taken into account. The layers are approximately 6.8 Å thick and are stacked parallel to the [010] direction, with successive layers being displaced by *c*/2 along [001].

Table 3
Selected bond lengths (Å), angles (deg.) and bond valence sums (v.u) for $[Ge(C_2N_2H_8)_3][GeSb_2S_6]$.

Atoms	Bond distances	v^a	Atoms	Bond distances	v^a
Sb(1)–S(2)^{i}	2.468(1)	0.95	Ge(1)–S(1)	2.136(2)	1.26
Sb(1)–S(4)	2.459(1)	0.98	Ge(1)–S(2)	2.247(1)	0.93
Sb(1)–S(5)	2.427(1)	1.06	Ge(1)–S(3)	2.214(1)	1.02
	Sum	2.99	Ge(1)–S(4)	2.262(1)	0.89
				Sum	4.10
Sb(2)–S(3)	2.759(1)	0.43	Ge(2)–N(1)	2.192(5)	0.43
Sb(2)–S(5)	2.464(2)	0.96	Ge(2)–N(2)	2.218(5)	0.40
Sb(2)–S(6)	2.388(1)	1.18	Ge(2)–N(3)	2.213(5)	0.41
Sb(2)–S(6)^{ii}	2.694(1)	0.52	Ge(2)–N(4)	2.215(5)	0.41
	Sum	3.09	Ge(2)–N(5)	2.197(5)	0.42
			Ge(2)–N(6)	2.239(5)	0.38
				Sum	2.45
S(2)^{i}–Sb(1)–S(4)	91.45(5)		S(1)–Ge(1)–S(2)	109.99(6)	
S(2)^{i}–Sb(1)–S(5)	89.87(5)		S(1)–Ge(1)–S(3)	115.92(6)	
S(4)–Sb(1)–S(5)	100.68(6)		S(1)–Ge(1)–S(4)	117.01(6)	
			S(2)–Ge(1)–S(3)	109.31(6)	
S(3)–Sb(2)–S(5)	91.71(4)		S(2)–Ge(1)–S(4)	101.53(6)	
S(3)–Sb(2)–S(6)	83.59(4)		S(3)–Ge(1)–S(4)	101.86(5)	
S(3)–Sb(2)–S(6)^{ii}	170.45(4)				
S(5)–Sb(2)–S(6)	102.57(5)				
S(5)–Sb(2)–S(6)^{ii}	85.14(5)				
S(6)–Sb(2)–S(6)^{ii}	88.29(4)				

Note: Symmetry transformations used to generate equivalent atoms: $^{i}x+\frac{1}{2}, y, \frac{1}{2}-z$; $^{ii}-x, -y, -z$.

[a] Bond valences calculated using data in Ref. [34].

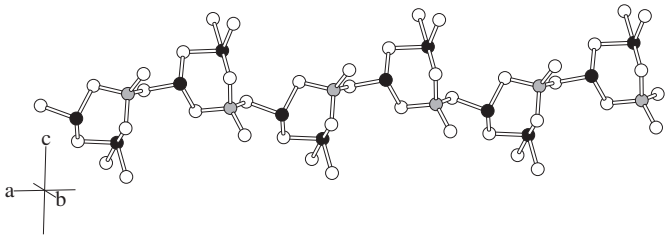

Fig. 2. A $GeSb_2S_7$ chain directed parallel to [100] constructed from linkage of six-membered germanium–antimony sulphide rings. Key: germanium, large shaded circles; antimony, large black circles; sulphur, large open circles.

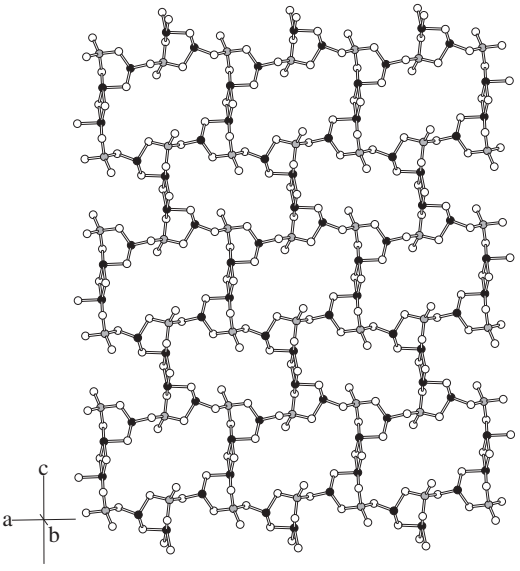

Fig. 3. View onto the (010) crystallographic plane of a single $[GeSb_2S_6]^{2-}$ layer generated by linking $GeSb_2S_7$ chains through Sb_2S_2 rings. Key as for Fig. 2.

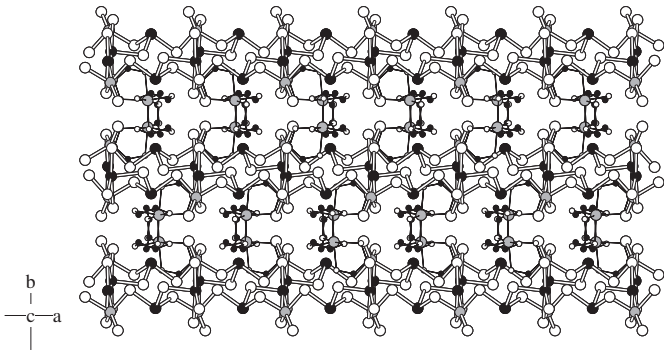

Fig. 4. View along the [001] direction illustrating the location of the charge balancing $Ge(en)_3^{2+}$ cations between $[GeSb_2S_6]^{2-}$ layers. Key: germanium, large shaded circles; antimony, large black circles; sulphur, large open circles; carbon, small black circles; nitrogen, small open circles. Hydrogen atoms of the ethylenediamine ligands are omitted for clarity.

Bond-valence sums [35] are consistent with the formal oxidation states Sb(III) and Ge(IV). This results in the germanium–antimony sulphide layers being doubly negatively charged. Charge-balancing is provided by a cationic coordination complex of Ge(2) located between the $[GeSb_2S_6]^{2-}$ layers (Fig. 4). Bond-valence sums indicate that it is divalent, $[Ge(en)_3]^{2+}$. Consequently in addition to possessing a mixed-metal framework, the title compound also contains germanium in two oxidation states. The charge-balancing $[Ge(en)_3]^{2+}$ cations are located between the $[GeSb_2S_6]^{2-}$ layers and form zigzag chains of cations directed along the [100], with neighbouring germanium centres being related by the two-fold screw axis along the *a* direction. Cations with $\Delta(\delta\delta\lambda)$ and $\Lambda(\lambda\lambda\delta)$ conformations are present as a result of the centrosymmetric nature of the structure; the material is therefore achiral. The distances between nitrogen atoms of the $[Ge(en)_3]^{2+}$ complex and sulphur atoms of the $[GeSb_2S_6]^{2-}$ layers (Table S1 of the Supplementary materials) lie in the range 3.34–3.69 Å, suggesting an extensive network of hydrogen bonds between the cationic complex and the thiometallate layers (Figure S4 of the Supplementary materials).

The band gap determined by optical spectroscopy is 2.49(4) eV (Fig. 5). Through analysis of a large body of experimental data, we have identified [15] in antimony sulphides, a correlation between the optical band gap and the framework density, expressed as the number of antimony atoms per 1000 Å^3. In particular, there is a near-linear relationship (Fig. 6) between optical band gap and framework density that holds remarkably well for antimony sulphides with a wide range of structures, regardless of the dimensionality of the antimony–sulphur framework.

The origin of this correlation lies in the nature of the electronic states in the vicinity of the Fermi level. Band structure calculations [36] for the binary sulphide, Sb_2S_3, which comprises double Sb_4S_6 chains of edge-linked SbS_5 square-based pyramids and SbS_3 trigonal pyramids, indicate that the optical band gap corresponds to a transition between states of predominantly sulphur 3*p*-character in the lower valence band and states in the upper conduction band deriving from an admixture of Sb 5*s*/*p*-type levels with sulphur *p*-levels. X-ray photoelectron spectroscopy measurements [37] reveal that the highest energy valence-band levels of Sb_2S_3 derive from sulphur 3*p* lone pairs. The presence of a valence band of predominantly sulphur character separated by a band gap from a conduction band principally of antimony character appears to be preserved in more complex quaternary antimony sulphides [38]. This suggests that the optical band gap in thioantimonates may be generally associated with a transition from valence band levels of sulphur 3*p* character. In Sb_2S_3, the levels closest to the Fermi energy arise from the interaction of sulphur 3*p* levels with antimony 5*s* levels. Decreasing the number

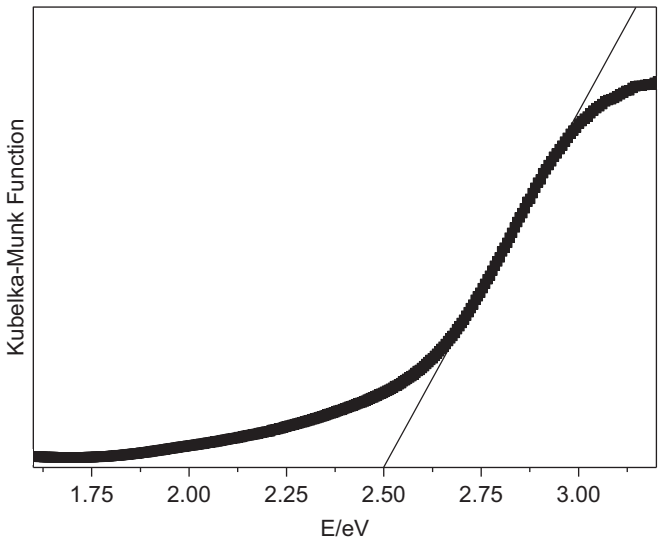

Fig. 5. Diffuse reflectance spectrum of $[Ge(C_2N_2H_8)_3][GeSb_2S_6]$. The solid line shows the extrapolation through the linear portion of the band edge used to determine the band gap.

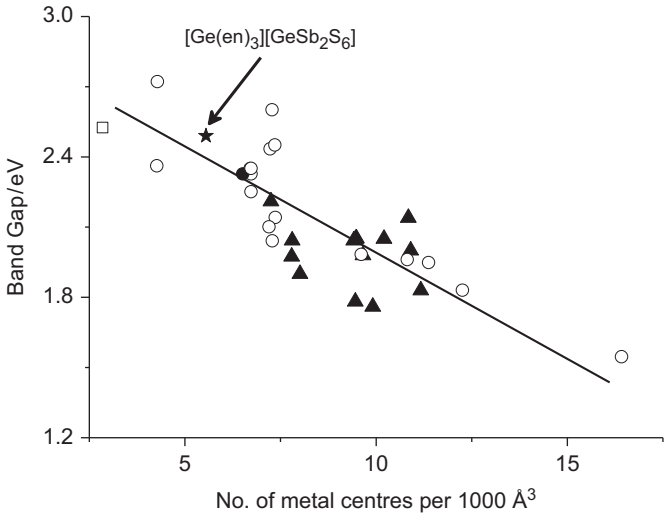

Fig. 6. A comparison of the optical band gap of $[Ge(C_2N_2H_8)_3][GeSb_2S_6]$ with those of thioantimonates of varying dimensionality. The band gap of the bimetallic thiometallate is indicated. The data demonstrate that the correlation between band gap and framework density established for the thioantimonates holds for the mixed-metal system reported here. The data used to construct this figure are presented as supplementary information to Ref. [16]. Key: open square, discrete unit; open circles, chain structures; solid triangles, layered structures; solid circle, three-dimensional structure. The solid line is a guide to the eye.

of antimony centres per unit volume weakens these interactions. This produces a contraction of the tail on the low-binding energy side of the valence band. Consequently, the increase in band gap with decreasing framework density observed in the thioantimonates may be associated with a narrowing of the valence band due to a decreased overlap of the sulphur lone pairs with antimony 5*s* levels.

The question arises as to the effect on the optical band gap of the introduction of a second metal into the metal–sulphur matrix. In the case of $[Ge(C_2N_2H_8)_3][GeSb_2S_6]$ reported here, the density of main-group metal atoms within the metal–sulphide matrix is 5.55 (Ge/Sb) atoms per 1000 Å^3. If the correlation we have previously identified for thioantimonates and discussed above holds, we would expect, for this framework density, a band gap

in the range 2.3–2.6 eV. As is evident from Fig. 6, the observed band gap of 2.49(4) eV is in excellent agreement with this prediction. This suggests that the presence of germanium does not significantly perturb the band structure in the region of the Fermi level, from that of the thioantimonates, and that states close to the top of the valence band remain predominantly of sulphur 3*p* character derived from sulphur lone pairs.

Bimetallic main-group thiometallates are a comparatively unexplored class of compounds [24,25,39,40]. Recent work [24,25] indicates that germanium–antimony sulphides may exhibit considerable structural diversity with materials containing discrete clusters, one-dimensional chains, two dimensional layers and three-dimensional frameworks all having been prepared. Of these materials, $M(en)_3[GeSb_2S_6]$ (M=Co, Ni) [25] contains the same layers as those of the title compound, suggesting that the six-membered $GeSb_2S_3$ heteroring may prove to be an important building unit in the construction of mixed-metal systems. Six-membered heterorings are also present in the recently reported $((CH_3)_2NH_2)[Ga_2Sb_2S_7]$ [22,23] and $(Haep)_2[Ga_2Sb_2S_7]$ [41] (aep=1-(2-aminoethyl)piperazine), each of which contains $Ga_2Sb_2S_7^{2-}$ layers interleaved with organic cations. However in these materials the heterorings, from which the layers are constructed, consist of two GaS_4 tetrahedra and one SbS_3 trigonal pyramid, giving them a composition of Ga_2SbS_3. Moreover, in contrast to the $GeSb_2S_3$ heterorings identified here, which are linked into layers by exocyclic sulphur atoms, pairs of gallium–antimony sulphide heterorings are fused *via* the Ga–S–Ga edge formed by the two vertex linked GaS_4 tetrahedra to form a larger $Ga_2Sb_2S_9$ building unit.

The observation of germanium in both the +2 and +4 oxidation states is perhaps the most remarkable feature of the title compound. In common with other post-transition-series elements, in addition to the group oxidation state, N, the $N-2$ oxidation state may arise from the so-called "inert-pair effect", the lower oxidation state becoming more stable on descending a given group. In group 14, the $N-2$ oxidation state is commonly observed for the heavier congeners tin and lead, whereas divalent Si(II) species are thermodynamically unstable under ambient conditions. Germanium appears to be an intermediate case, suggesting that the stability of the Ge(II)/Ge(IV) valence states is finely balanced. In the title compound, Ge(1) is coordinated by four sulphur atoms and, as always in such an environment, is tetravalent. Divalent germanium is generally associated with a higher coordination number. For example, in GeF_2, the local geometry about Ge is a distorted trigonal bipyramid, whilst in GeX_2 (X=Br, I) and the binary chalcogenides GeQ (Q=S, Se), the germanium has a highly distorted octahedral coordination [42]. The coordination chemistry of Ge(II) is relatively unexplored, although molecular complexes containing divalent Ge with nitrogen donor ligands have been reported, including $[Ge_2(py^*)_3][GeCl_3]$ (py^*=pyrazolyl) [43] and $[Ge(OH)_6][Ge(en)_3]$ [44]. Significantly in the context of the work reported here, Pell and Ibers [45] have described a selenoantimonate, $[Ge(en)_3][enH][SbSe_4]$ that contains the $[Ge(en)_3]^{2+}$ cationic complex. The present work thus appears to be only the second such report of the divalent Ge(2) tris-ethylenediamine complex serving as the charge-balancing counter ion to a chalcometallate framework. Materials containing germanium in intermediate oxidation states, such as Ge_5F_{12}, have been shown to be mixed valent. Similarly the ternary chalcogenides $Tl_2Ge_2S_4$ [46] and $Ba_2Ge_2Se_5$ [47] contain both Ge^{2+} and Ge^{4+}. Recently $[Mn(en)_3]_2[Ge_5Te_{10}]$ was prepared under solvothermal conditions [48] and shown to contain Ge(II), Ge(III) and Ge(IV). The ability to access lower (and mixed) oxidation states of germanium using the relatively mild conditions of solvothermal reactions suggests considerable scope for the development of the chemistry of mixed-valent germanium.

Supplementary information

Crystallographic data in CIF format, thermogravimetric data, powder X-ray diffraction data and a table of hydrogen bonds, together with an accompanying figure, for $[Ge(C_2N_2H_8)_3][GeSb_2S_6]$, are available.

Crystallographic data for the structure reported in this paper have been deposited at the Cambridge Crystallographic Data Centre: CCDC number 831958.

Acknowledgments

We thank the UK EPSRC for financial support through Grant EP/E056709.

Appendix A. Supplementary materials

Supplementary data associated with this article can be found in the online version at doi:10.1016/j.jssc.2011.09.032.

References

[1] R.L. Bedard, S.T. Wilson, L.D. Vail, J.M. Bennet, E.M. Flanigen, Zeolites: Facts, Figures, Future, in: P.A. Jacobs, R.A. Santen (Eds.), Elsevier, Amsterdam, 1989.
[2] (a) W.S. Sheldrick, M. Wachhold, Coord. Chem. Rev. 176 (1998) 211;
(b) J. Li, Z. Chen, R.J. Wang, D.M. Proserpio, Coord. Chem. Rev. 190–192 (1999) 707;
(c) A. Kromm, T.v. Almsick, W.S. Sheldrick, Z. Naturforsch. B. 65 (2010) 918;
(d) B. Seidlhofer, N. Pienack, W. Bensch, Z. Naturforsch. B. 65 (2010) 937.
[3] J. Zhou, J. Dai, G.-Q. Bian, C.-Y. Li, Coord. Chem. Rev. 253 (2009) 1221.
[4] T. Jiang, G.A. Ozin, J. Mater. Chem. 8 (1998) 1099.
[5] D.-X. Jia, J. Dai, Q.-Y. Zhu, L.-H. Cao, H.-H. Lin, J. Solid State Chem. 178 (2005) 874.
[6] X. Bu, N. Zheng, P. Feng, Chem. Eur. J. 10 (2004) 3356.
[7] P. Vaqueiro, M.L. Romero, J. Am. Chem. Soc. 130 (2008) 9630.
[8] P. Vaqueiro, Dalton Trans. 39 (2010) 5965.
[9] (a) M. Schur, A. Gruhl, C. Näther, I. Jess, W. Bensch, Z. Naturforsch. B 54 (1999) 1524;
(b) V. Spetzler, R. Kiebach, C. Näther, W. Bensch, Z. Anorg. Allg. Chem. 630 (2004) 2398;
(c) J.B. Parise, Y. Ko, Chem. Mater. 4 (1992) 1446;
(d) K. Tan, Y. Ko, J.B. Parise, J.H. Park, A. Darovsky, Chem. Mater. 8 (1996) 2510;
(e) R.J.E. Lees, A.V. Powell, A.M. Chippindale, Acta Crystallogr. Sect. C 61 (2005) m516;
(f) K. Tan, Y. Ko, J.B. Parise, Acta Crystallogr. Sect. C 50 (1994) 1439.
[10] (a) R. Stähler, C. Näther, W. Bensch, J. Solid State Chem. 174 (2003) 264;
(b) A.V. Powell, S. Boissiére, A.M. Chippindale, Chem. Mater. 12 (2000) 182.
[11] P. Vaqueiro, A.M. Chippindale, A.V. Powell, Inorg. Chem. 43 (2004) 7963.
[12] A.V. Powell, R.J.E. Lees, A.M. Chippindale, Inorg. Chem. 45 (2006) 4261.
[13] H.A. Graf, H. Schaefer, Z. Naturforsch. B 27 (1972) 735.
[14] W.M. Hutchinson, A.R. Collett, C.L. Lazzell, J. Am. Chem. Soc. 67 (1945) 1966.
[15] A.V. Powell, R. Paniagua, P. Vaqueiro, A.M. Chippindale, Chem. Mater. 14 (2002) 1220.
[16] A.V. Powell, R.J.E. Lees, A.M. Chippindale, J. Phys. Chem. Solids 69 (2008) 1000.
[17] M. Schaefer, R. Stähler, W.R. Kiebach, C. Näther, W. Bensch, Z. Anorg. Allg. Chem. 630 (2004) 1816.
[18] R. Stähler, W. Bensch, Eur. J. Inorg. Chem. (2001) 3073.
[19] R. Kiebach, W. Bensch, R.D. Hoffmann, R. Pöttgen, Z. Anorg. Allg. Chem. 629 (2003) 532.
[20] M. Schur, W. Bensch, Z. Naturforsch. B 57 (2002) 1.
[21] N. Ding, M.G. Kanatzidis, Chem. Mater. 19 (2007) 3867.
[22] J.L. Mertz, N. Ding, M.G. Kanatzidis, Inorg. Chem. 48 (2009) 10898.
[23] M.-L. Feng, Z.L. Xie, X.-Y. Huang, Inorg. Chem. 48 (2009) 3904.
[24] N. Ding, M.G. Kanatzidis, Nat. Chem. 2 (2010) 187.
[25] M.-L. Feng, D.-N. Kong, Z.-L. Xie, X.-Y. Huang, Angew. Chem. Int. Ed. 47 (2008) 8623.
[26] M.-L. Feng, W.-W. Xiong, D. Ye, J.-R. Li, X.-Y. Huang, Chem. Asian J. 5 (2010) 1817.
[27] W.W. Wendlandt, H.G. Hecht, Reflectance Spectroscopy, Interscience Publishers, New York, 1966.
[28] Apex-2 Software, Bruker-AXS, Madison, Wisconsin, USA, 2004.
[29] A. Altomare, G. Cascarano, C. Giacovazzo, A. Guangliardi, M. Burla, G. Polidori, M. Camalli, J. Appl. Crystallogr. Sect. A 27 (1994) 435.

[30] P.W. Betteridge, J.R. Carruthers, R.I. Cooper, C.K. Prout, D.J. Watkin, J. Appl. Cryst. 36 (2003) 1487.
[31] A. Bondi, J. Phys. Chem. 68 (1964) 441.
[32] K. Volk, P. Bickert, R. Kolmer, H. Schäfer, Z. Naturforsch. B 34 (1979) 380.
[33] L. Engelke, C. Näther, W. Bensch, Eur. J. Inorg. Chem. (2002) 2936.
[34] A. Puls, M. Schaefer, C. Näther, W. Bensch, A.V. Powell, S. Boissière, A.M. Chippindale, J. Solid State Chem. 178 (2005) 1171.
[35] N.E. Brese, M. O'Keeffe, Acta Crystallogr. B47 (1991) 192.
[36] A.G. Khasabov, I.Y. Nikiforov, Sov. Phys. Crystallogr. 16 (1971) 28.
[37] P.E. Lippens, J. OlivierFourcade, J.C. Jumas, A. Gheorghiu, S. Dupont, C. Sénémaud, Phys. Rev. B 56 (1997) 13054.
[38] B. Deng, G.H. Chan, D.E. Ellis, R.P. Van Duyne, J.A. Ibers, J. Solid State Chem. 178 (2005) 3169.
[39] J.A. Zhou, X.H. Yin, F. Zhang, Inorg. Chem. 49 (2010) 9671.
[40] J.A. Zhou, L.T. An, F. Zhang, Inorg. Chem. 50 (2011) 415.
[41] Z. Lin, X. Bu, P. Feng, Micropor. Mesopor. Mater. 132 (2010) 328.
[42] A.F. Wells, Structural Inorganic Chemistry, 5th Edition, Oxford University Press, Oxford, 1984.
[43] B. Kersting, B. Krebs, Inorg. Chem. 33 (1994) 3886.
[44] F. Gándara, M.E. Medina, N. Snejko, B. Gómez-Lor, M. Iglesias, E. Gutiérrez-Puebla, M. Angeles Monge, Inorg. Chem. 47 (2008) 6791.
[45] M.A. Pell, J.A. Ibers, Inorg. Chem. 35 (1996) 4559.
[46] G. Eulenberger, J. Less Common. Met. 108 (1985) 65.
[47] D. Johnrendt, M. Tampier, Chem. Eur. J. 6 (2000) 994.
[48] Q. Zhang, G. Armatas, M.G. Kanatzidis, Inorg. Chem. 48 (2009) 8665.